Topology Generation for Hybrid Electric Vehicle Architecture Design

Alparslan Emrah Bayrak*

Mechanical Engineering
University of Michigan
Ann Arbor, MI 48109
Email: bayrak@umich.edu

Yi Ren

Mechanical Engineering
Arizona State University
Tempe, Arizona, 85287
Email: yiren@asu.edu

Panos Y. Papalambros

Mechanical Engineering
University of Michigan
Ann Arbor, MI 48109
Email: pyp@umich.edu

Existing hybrid powertrain architectures, i.e., the connections from engine and motors to the vehicle output shaft, are designed for particular vehicle applications, e.g., passenger cars or city buses, to achieve good fuel economy. For effective electrification of new applications (e.g., heavy-duty trucks or racing cars), new architectures may need to be identified to accommodate the particular vehicle specifications and drive cycles. The exploration of feasible architectures is combinatorial in nature and is conventionally based on human intuition. We propose a mathematically rigorous algorithm to enumerate all feasible powertrain architectures, therefore enabling automated optimal powertrain design. The proposed method is general enough to account for single and multi-mode architectures as well as different number of planetary gears and powertrain components. We demonstrate through case studies that our method can generate the complete sets of feasible designs, including the ones available in the market and in patents.

1 Introduction

Increasing demand on energy efficiency has motivated expansion of powertrain electrification from passenger cars to buses [1, 2] and other utility vehicles [3, 4]. One critical design decision to make in the electrification process is the *configuration* of the powertrain, which defines connection arrangements among powertrain components and thus the dynamics and the powertrain efficiency. While a powertrain design can have a single configuration, other powertrain designs switch among multiple configurations during vehicle operation, such as the Chevrolet Volt, see Figure 1. Disengaging Clutch 1 (CL1) and engaging CL2 of the powertrain in this figure gives a hybrid configuration (Figure 1a), while engaging or disengaging both CL1 and CL2 achieves pure electric configurations (Figures 1b, 1c). The collection of all configurations in the design defines the *architecture* of a powertrain. Architectures with more than one configuration are called multi-mode architectures and each particular configuration is called a *driving mode*. Switching among multiple configurations allows the powertrain to achieve better performance and fuel economy under changing driving conditions. While available powertrain architectures in the market have achieved significant fuel efficiency, these are designed for the given vehicle specifications and design requirements, and may not perform well or even be feasible when the vehicle specifications or driving conditions change [5].

Configuration design has been studied in other domains including the design of structural systems [6, 7], kinematic chains [8, 9], electrical circuits [10] and chemical molecules [11]. There are also general configuration synthesis approaches that apply to various design domains relying on a given library of components [12–14]. The combinatorial nature of powertrain architecture design requires one to enumerate and identify all feasible configurations to determine the optimal design. In the conventional powertrain design domain, methods have been developed to create all possible design alternatives for 4-speed [15] and 6-speed [16] automatic transmissions. However, methodologies in most these studies remain limited to their specific domain. Domain independent approaches cannot capture the kinematic feasibility constraints essential in planetary gear systems. Thus, hybrid powertrain architectures require a different ap-

*Address all correspondence to this author.

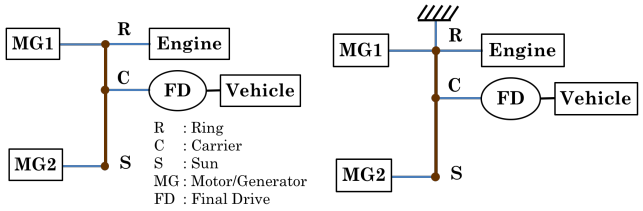

(a) Hybrid configuration

(b) First pure electric configuration

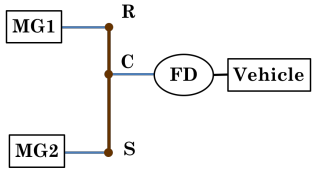

(c) Second pure electric configuration

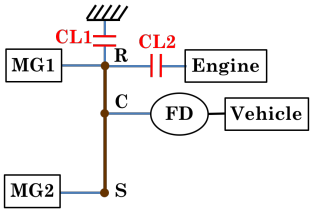

(d) Combined multi-mode architecture

Fig. 1: Lever representation of three modes of a modified Chevrolet Volt architecture (without series hybrid mode)

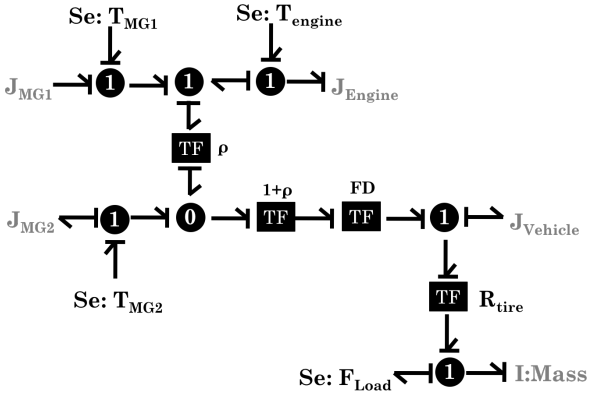

(a) Original bond graph representation of the hybrid configuration of the Chevrolet Volt architecture

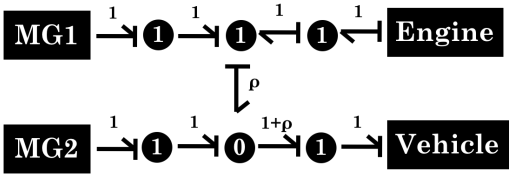

(b) Modified bond graph representation of the hybrid configuration of the Chevrolet Volt architecture

Fig. 2: Representation of the hybrid configuration of the Chevrolet Volt architecture in Figure 1a

proach. Due to the large number of possible configurations with one Planetary Gear (PG) [17, 18], 2 PGs [19–23] and 3 PGs [24, 25], existing hybrid powertrain design research has focused on subsets of the overall design space, e.g., enumeration of 1- and 2-PG configurations [5], exploration of the Toyota Prius-like designs [26], and variations of a baseline configuration [27]. A recent study by Zhang et al. proposes a power-split hybrid architecture design framework to select configurations by designing the system configuration matrix [28]. The framework relies on a commonly used set of powertrain components, i.e. a single engine and two motor/generators.

This article proposes a general systematic approach to generate all feasible hybrid and pure electric configurations with an arbitrary number of PGs and any set of powertrain components. The generation process uses a modified bond graph representation of powertrain configurations. An earlier version of this work appeared in [29]. The generation method is combined with a search in the feasible space of configurations to identify promising design candidates. A sequel to the present article [30, 31] offers an example for such a design methodology.

In Section 2, we describe the proposed representation of powertrain configurations. In Section 3 we formulate the process for generating all feasible configuration alternatives using this representation. Section 4 describes the creation of multi-mode architectures by combining the generated configurations. In Section 5 we discuss results and in Section 6 we offer conclusions.

2 Representation of HEV Configurations

Due to the combinatorial nature of configuration optimization, finding a globally optimal design requires a systematic approach to generating all feasible design alternatives. A formal representation of powertrain configurations is necessary for such a generation method. Current studies have utilized a variety of powertrain representations for visualization and analysis purposes. These include stick diagrams as commonly seen in patents, lever diagrams [32], canonical graphs [33], dynamic system matrices [5], and bond graphs [29, 34]. Each of these representations has advantages and disadvantages determining the computational effort required to generate the feasible design space of powertrain configurations. In this article we use bond graphs since they provide built-in tools to model the power flow and allow us to check the feasibility of a powertrain configuration by the use of causality rules. Other graphical representations require additional calculations to model the power flow that is used to determine the kinematic degree of freedom of a configuration. It acts as another feasibility constraint as discussed in Section 3.4.

This section introduces a modified bond graph representation specifically tailored for generating powertrain configurations. We also introduce connectivity tables extracted from the bond graphs to be used for creating multi-mode architectures.

2.1 Modified Bond Graph Representation

Bond graphs are graphical models that specify the power flow in a dynamic system [35]. Their application in modeling HEV powertrain systems is explained in Figure 2, where the dynamics of the hybrid configuration of the Chevrolet Volt architecture is captured by a bond graph. The key element in this architecture is the PG set represented by a lever in Figure

1a where R denotes the ring, C the carrier and S the sun gear. In steady state, the gear speed relationship is :

$$(1+\rho)\omega_c = \rho\omega_r + \omega_s, \tag{1}$$

where ρ is the ring to sun gear ratio, and ω_c, ω_r, ω_s denote the speeds of the carrier, ring and sun gears, respectively. Taking the particular component arrangement of this powertrain into account, the speed relationship can be rewritten in the following matrix form:

$$\begin{bmatrix} 1 & 0 \\ -\rho & (1+\rho) \end{bmatrix} \begin{bmatrix} \omega_{eng} \\ \omega_{out} \end{bmatrix} = \begin{bmatrix} \omega_{MG1} \\ \omega_{MG2} \end{bmatrix}. \tag{2}$$

Here, ω_{eng}, ω_{MG1}, ω_{MG2} and ω_{out} are speeds of the engine, Motor/Generators 1 and 2 (MG1, MG2), and output shaft to the final drive, respectively. The bond graph model shown in Figure 2a models this kinematic relationship as well as the corresponding torque relationship ignoring gear losses and gear inertia. A 0-junction imposes all torques around the junction to be the same while the sum of the speeds to be equal to zero. In our particular application, a 0-junction is used to model the kinematic relationship among different gears of a PG set given in Equation (1). In case of 1-junction, torque and speed relationships of a 0-junction are swapped. Physically a 1-junction models the relationship of the components connected to the same gear of PG set. Engine, MGs and vehicle output are modeled as effort sources denoted as "Se" in the figure. The transformer blocks denoted as "TF" are used to model the gear ratios and the tire radius. Since the losses are ignored, the following toque relationship can be derived from the conservation of power.

$$-\begin{bmatrix} 1 & 0 \\ -\rho & (1+\rho) \end{bmatrix}^{-T} \begin{bmatrix} T_{eng} \\ -T_{out} \end{bmatrix} = \begin{bmatrix} T_{MG1} \\ T_{MG2} \end{bmatrix}. \tag{3}$$

Two simplifications to the bond graph representation can be made in the current context: First, bond graphs for fixed powertrain components (i.e., engine, MGs, output shaft, and ground) are simplified as flow and effort sources (or sinks), and are referred to as *external components*. Second, transformer blocks can be represented as bond weights and weight is set to 1 if no transformer exists between two adjacent junctions. The representation after these simplifications is a *modified bond graph*. Figure 2b shows the modified bond graph representation of the hybrid configuration in the Chevrolet Volt architecture. Further, we refer to the junctions connected to the external components as *external junctions* and the rest as *internal* ones. The number of external junctions is equal to that of external components. We show in Section 3 that PGs can be represented by internal junctions, and the number of internal junctions corresponds to the number of PGs. It should be noted that each bond graph represents a single configuration. Separate bond graphs are needed in a multi-mode architecture.

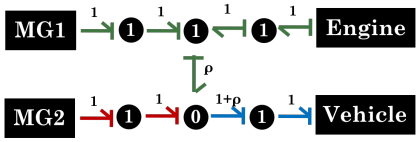

	S1	R1	C1
Engine	0	0	1
Vehicle	0	1	0
MG1	1	0	0
MG2	0	1	0
Ground	0	0	0
S1	0	0	0
R1	0	0	0
C1	0	0	0

Fig. 3: Example of a modified bond graph representation and its connectivity table (best viewed in color)

2.2 Connectivity Table

Recall that multi-mode architectures (i.e., combination of multiple bond graphs) are often necessary for improving fuel economy in various driving conditions, with switching among configurations enabled by a clutch mechanism. For the representation to be physically meaningful during design optimization, we must calculate the number of clutches needed to enable the switching in a given architecture. To facilitate this calculation (see details in Section 4), we introduce a *connectivity table*, i.e., a binary matrix that defines the connections among powertrain components and each particular gear in a PG system. The size of the connectivity table for a general case is $(N_{ext} + 3N_{PG}) \times 3N_{PG}$ where N_{ext} is the number of external components and N_{PG} is the number of planetary gears in the system. The first N_{ext} rows define the connections from the external components to the PG system while the remaining $3N_{PG}$ rows define internal connections among the PGs. For example, the connectivity table corresponding to the hybrid configuration of the Chevrolet Volt architecture is given in Figure 3. Since it is a 1-PG system, the last three rows are all zeros.

The connectivity table can be seen as the matrix form of the "simple" lever representation (i.e., lever diagrams with three nodes), while the so-called "compound" levers (i.e., diagrams with more than three nodes, see [32] for example) are commonly used to represent multiple-PG systems. Nonetheless, each compound lever corresponds to a combination of simple levers. Thus, we can standardize the size of the connectivity table based on the number of external components and PGs involved in the system.

3 Configuration Generation

In this section we describe the automated process to generate all feasible powertrain configurations. Figure 4 summarizes the process: We first generate all simple, connected, and undirected graphs based on the external components and number of PGs. Then, we assign junction types and causalities to convert the undirected graphs to bond graphs. Finally, we assign the graph weights to every bond in order to represent a PG system. Once a bond graph corresponding to a configuration is created, the quasi-static system of equations is extracted and exported to a vehicle model for design evaluation.

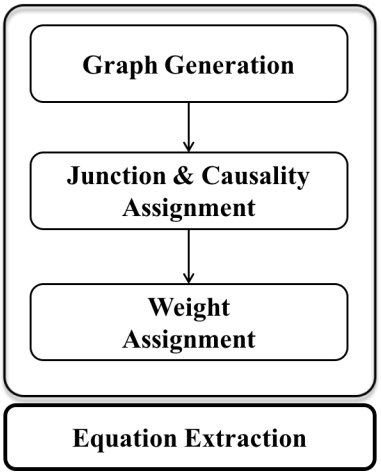

Fig. 4: Configuration generation process flow

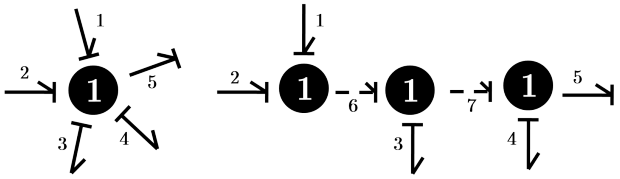

Fig. 5: A junction with 5 bonds is equivalently replaced by 3 junctions with 3 bonds each

The following bond graph properties will help us in formulating the generation process.

Property 1. *A valid bond graph must be simple and connected.*

A simple graph does not have more than one bond between any pair of junctions and contains no loops around a single junction, i.e., a junction is not directly connected to itself. Also, in a connected graph no junction remains disconnected.

Property 2. *A junction with $n > 3$ bonds is equivalent to $n-2$ junctions of the same type with three bonds each.*

In the original bond graph representation, a junction can have any number of bonds connected to it. However, in this study, we restrict the internal junctions to have three bonds and external junctions to have one bond connected to an internal junction for simpler implementation. This property shows that such a restriction does not limit modeling capabilities. Figure 5 explains this property for a 1-junction with 5 bonds: In a chain of bonds, both the first and last junctions will have two bonds from the original model, leaving $n-4$ bonds for the remaining junctions. Each intermediate junction can only have one bond from the original model, since two bonds are needed to connect to other junctions. Therefore, in total $2+(n-4) = n-2$ junctions are needed to represent the original model.

Property 3. *A bond graph must have an even number of junctions if each internal junction has three bonds and each external one has one bond connected to an internal junction.*

From Properties 1 and 2, a bond graph with J^{ext} number of external junctions and J internal junctions has $(3J - J^{ext})/2 + J^{ext}$ bonds. Since the number of bonds has to be an integer, $3J - J^{ext}$, or equivalently $J + J^{ext}$, must be even.

Property 4. *The number of 0-junctions is equal to the number of PGs in the system.*

Since we restricted the number of bonds around a junction to three, a separate 0-junction is necessary to represent the kinematic relationship among sun, ring and carrier gears given in Equation (1) for each PG system. Note that if our restriction on number of bonds is relaxed, the systems where two or more 0-junctions are connected to each other can be represented a single 0-junction. This restriction makes formulating the graph generation problem easier.

A step-by-step bond graph generation process is described as follows.

3.1 Graph Generation

We start with generating simple, connected, undirected graphs. Recall that each external junction is connected to an external component and the number of external components is usually small. In a typical hybrid powertrain, the external components are an engine, two MGs, one vehicle output and a ground. Here, ground refers to an immobile node that is generally achieved by connecting a gear to the stationary housing frame. Four types of configurations can be defined in this context: (1) Hybrid with ground, (2) hybrid without ground, (3) pure electric with engine engaged, (4) pure electric without engine. The first two are the configurations in which the engine actively provides motive power to the system. The only difference between them is that the former has one of the PG nodes connected to a fixed ground, providing zero speed. In (3) and (4), the engine is deactivated by either being connected to a fixed ground or being disconnected from the system by a clutch, respectively. Connecting a PG node to ground may allow the architecture to achieve higher torque outputs. The output torque obtained at the vehicle shaft is constrained by the torque limitations of the powertrain components actively engaged in the architecture but a ground connection does not have any torque limitation. The study by Zhang et al. [26] can be given as an example exploiting this benefit of grounding in HEV architecture design.

Following the bond graph properties introduced earlier, Table 1 summaries the number of junctions needed for each type of configuration. Note that these numbers can be generalized to any set of external components and any number of PGs. We picked these cases as examples to demonstrate the application of the proposed methodology to designs in common practice.

Given the number of junctions, let $\mathbf{G}_{(J^{ext}+J)\times(J^{ext}+J)} = [\mathbf{0}\ \mathbf{A}; \mathbf{A^T}\ \mathbf{B}]$ be the adjacency matrix representing a graph where $\mathbf{A}_{J^{ext}\times J}$ and $\mathbf{B}_{J\times J}$ are binary matrices. The matrix $\mathbf{A}$ represents the connections between external and internal junctions and $\mathbf{B}$ represents the connections among internal

Table 1: Number of junctions needed for one engine, two MGs and one ground

Number of PGs	HEV Mode without Ground	HEV Mode with Ground	Pure EV Mode with Engine	Pure EV Mode without Engine
1-PG	$J^{ext} = 4$, $J = 2$	– –	$J^{ext} = 5$, $J = 3$	$J^{ext} = 3$, $J = 1$
2-PG	$J^{ext} = 4$, $J = 4$	$J^{ext} = 5$, $J = 3$	$J^{ext} = 5$, $J = 3$ or 5	$J^{ext} = 3$, $J = 3$
3-PG	$J^{ext} = 4$, $J = 6$	$J^{ext} = 5$, $J = 5$	$J^{ext} = 5$, $J = 5$ or 7	$J^{ext} = 3$, $J = 5$

junctions. The corresponding value in the matrix is 1 when there is a connection between two junctions and 0 otherwise. We can see that if the junctions i and j are connected, $B_{ij} = B_{ji} = 1$. Then, the matrix $\mathbf{B}$ is symmetric. Also the $\mathbf{0}_{J^{ext} \times J^{ext}}$ block in the adjacency matrix prevents any direct connection among external junctions.

The designs of matrices $\mathbf{A}$ and $\mathbf{B}$ determine the graph under the following constraints:

(i) An external junction must have only one bond:

$$\sum_{j=1}^{J} A_{ij} = 1, \qquad \forall i = 1,2,3,...,J^{ext}. \tag{4}$$

(ii) Each internal junction must have exactly 3 bonds:

$$\sum_{i=1}^{J^{ext}} A_{ij} + \sum_{i=1}^{J} B_{ij} = 3, \qquad \forall j = 1,2,3,...,J. \tag{5}$$

In order to enumerate all possible graphs satisfying the constraints given by Equations (4) and (5), all possible $\mathbf{A}$s are first enumerated from Equation (4). Then, for each enumerated $\mathbf{A}$, all possible $\mathbf{B}$s are found from Equation (5). Since J^{ext} and J do not take large values, i.e., the number of powertrain components is usually limited, the computational cost of this enumeration process is tractable.

The enumeration process described above might create replicated graphs with different ordering of junctions. Figure 6 shows such a case. By changing the labels of the junctions, the same systems can be obtained from each other. This phenomenon is known as graph isomorphism [36]. Isomorphism exists in any graphical representation and must be identified to eliminate the replicates. Algorithms exist to identify graph isomorphism, see for example [37, 38]. We use the available implementation of isomorphism detection named *graphisomorphism* in MATLAB [39] to filter the isomorphic graphs.

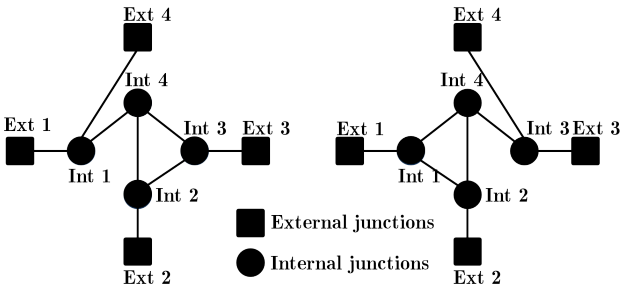

Fig. 6: Two replicates generated from the enumeration process. Both graphs result in the same equation sets after assigning the junction type and bond weights

3.2 Junction and Causality Assignment

After the enumeration of all undirected graphs with no replicates, it is necessary to assign 0- and 1-junctions to the nodes of the graphs. This assignment process is linked with the causal stroke assignment since the causality restricts the junction assignment. A causal stroke identifies the side of a bond that imposes flow (speed) on the system whereas effort (torque) is imposed by the side without a causal stroke. The assignment process starts with the external junction assignment. All external junctions are assigned to be 1-junctions. We also need to assign causalities to the internal junctions. It can be seen from Figure 2b that in a hybrid configuration the causality stroke is on the internal junction side for MG1 and MG2, and on the external junction side for engine, vehicle output. This assignment implies that engine and vehicle output impose speed on the system while MGs impose torque.

For pure electric modes the causality assignment of the engine (if it exists) is opposite since the engine is grounded. The ground imposes zero speed to the engine. The causality of one of MGs is also flipped as necessary to make the assignment consistent, i.e., the speed of one of the MGs is freely determined by the controller if the MG is not grounded.

The causality assignment employed here restricts some of the configurations. For instance, since engine and vehi-

cle output have the same causality, they can never be connected to the same gear of a PG set directly. However, such a configuration links the engine speed to the vehicle speed directly, leaving no possibility to control engine speed. Thus, these less efficient designs are not considered in the configuration generation stage. When the designs of interest include parallel configurations, the engine and output shaft must be allowed to be connected to the same node of PG set by flipping the causality of the engine. Recall that, in order to allow some variety of speed ratios, this design requires an additional transmission at the vehicle output.

Next, we assign junction types and causal strokes for the internal junctions. Let $\beta = (3J - J^{ext})/2$ denote the number of bonds connecting the internal junctions to each other. Also denote the junction type for the junction j as t_j. Let $t_j = 1$ when the junction type is 1 and $t_j = -1$ when the junction type is 0. This assignment is useful when formulating the junction type assignment problem. We denote the causality on the bond connecting the junctions j_1 and j_2 as $c_{j_1 j_2}$ and assign $c_{j_1 j_2} = 1$ if the stroke is on the junction j_1 side, implying $c_{j_2 j_1} = -1$. With these definitions and according to the bond graph rules, the following equation is stated:

$$-t_{j_1} + \sum_{j_2 | G_{j_1 j_2}=1} c_{j_1 j_2} = 0, \qquad \forall j_1 = 1,2,3,...,J. \quad (6)$$

Since the total number of equations is J and the number of unknowns to be determined is $\beta + J$, multiple solutions exist. Summing all the equations from Equation (6) gives:

$$\sum_{j_1=1}^{J} (-t_{j_1} + \sum_{j_2 | G_{j_1 j_2}=1} c_{j_1 j_2}) = 0. \quad (7)$$

The sum of all causalities between internal junctions is zero since for every $c_{j_1 j_2}$ there exists a $c_{j_2 j_1}$ such that $c_{j_1 j_2} + c_{j_2 j_1} = 0$. Therefore, sum of the junction types is equal to the sum of the causalities of the external bonds. This result leads to the number of junctions in Table 1, assuming that the powertrain consists of one engine, two MGs and one ground node. Combined with Property 4, we can determine how many 0- and 1-junctions to assign to the system. This enables the enumeration of all possible junction and causality assignments.

Note that in Table 1, under our causality assumptions for external components, it is not possible to obtain a feasible hybrid configuration with ground engaged among 1-PG designs. Also, for pure electric modes with the engine connected to the grounded gear, the number of internal junctions can take two different values, due to the causality assignment of the MGs. If one of the MGs is assigned to impose flow on the system, fewer internal junctions are required to make the bond graph feasible.

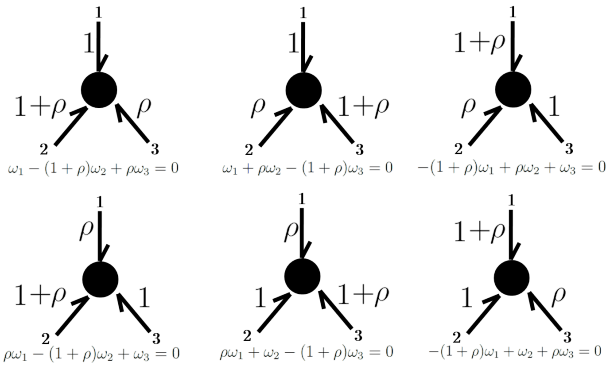

Fig. 7: All possible six combinations for the bond weight assignment around a 0-junction

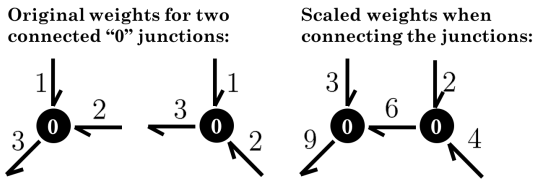

Fig. 8: Bond weight scaling for a 0- to 0-junction connection

3.3 Weight Assignment

In order to complete the modified bond graph enumeration process, the proper bond weights (weights for the TF blocks) that correspond to feasible configurations need to be assigned. Let ρ be the ring to sun PG ratio. As Figure 2b also shows, a PG set is modeled by 0- and 1-junctions together, with weights around a 0-junction being 1, ρ and $1+\rho$, and the rest of the bond weights being 1. There are six possible ways to assign these bond weights around a 0-junction as shown in Figure 7.

Assignment of bond weights must be consistent. When connecting two 0-junctions together, bond weight assignments might conflict and scaling of the weights might be necessary to resolve the conflict. Figure 8 shows an example for a 0-to-0 junction connection when scaling is needed. In the figure, the original bond weights connecting two 0-junctions, i.e., weights of 2 and 3, conflict with each other. These weights are scaled to the least common multiple of the conflicting bond weights. In this case, bond weights of the left junction are multiplied by 3 and those of the right junction are multiplied by 2.

3.4 Equation Extraction

Once enumeration and weight assignment are complete, the link between the graph representation and the system equations must be formed to evaluate the designs.

Let $\boldsymbol{\omega}^{ext}$ be the vector of speeds from external components. Define $\boldsymbol{\omega}$ as the $\beta \times 1$ vector of speeds on the bonds connecting internal junctions. Following the bond graph rules for 0- and 1-junctions, i.e., speeds around a 0-junction sum up to 0 and speeds around a 1-junction are the same, the

following system of equations can be written,

$$\mathbf{W_0}\boldsymbol{\omega}^{ext} + \mathbf{W}\boldsymbol{\omega} = 0, \tag{8}$$

where $\mathbf{W_0}$ and $\mathbf{W}$ are the matrices containing the bond weights from the graph. Let J_0 and J_1 denote the number of 0-junctions and 1-junctions, respectively. Then, $\mathbf{W}$ is a matrix of size $(J_0 + 2J_1) \times \beta$ since a 0-junction defines a single relationship for the speeds and 1-junction defines two. When $\mathbf{W}$ has rank β, Equation (8) can be rewritten as,

$$\boldsymbol{\omega} = -(\mathbf{W^T W})^{-1}\mathbf{W}^T\mathbf{W_0}\boldsymbol{\omega}^{ext}. \tag{9}$$

Substituting Equation (9) into Equation (8) gives:

$$(\mathbf{W_0} - \mathbf{W}(\mathbf{W^T W})^{-1}\mathbf{W^T W_0})\boldsymbol{\omega}^{ext} = \mathbf{0}. \tag{10}$$

Call $\widetilde{\mathbf{W}} = (\mathbf{W_0} - \mathbf{W}(\mathbf{W^T W})^{-1}\mathbf{W^T W_0})$ a matrix of size $(J_0 + 2J_1) \times J^{ext}$ that contains all linear kinematic equations relating all external components. The rank of $\widetilde{\mathbf{W}}$ that determines the kinematic degree of freedom (dof) of the PG system ranges from 1 to 3. From here, separate analyses need to be performed for hybrid and pure electric configurations.

(i) For hybrid configurations, a rearrangement is necessary to obtain the kinematic relationship matrix of Equation (10) in Section 2. Consider a specific case with $\boldsymbol{\omega}^{ext} = [\omega_1, \omega_2, \omega_3, \omega_4]$ being the vector of speeds from engine, vehicle output, MG1 and MG2, respectively. Let $[\widetilde{\mathbf{W}}_1, \widetilde{\mathbf{W}}_2] = \widetilde{\mathbf{W}}$, where both $\widetilde{\mathbf{W}}_1$ and $\widetilde{\mathbf{W}}_2$ are of size $(J_0 + 2J_1) \times 2$. When both $\widetilde{\mathbf{W}}_2^T\widetilde{\mathbf{W}}_1$ and $\widetilde{\mathbf{W}}_2^T\widetilde{\mathbf{W}}_2$ are invertible, rearrangement on Equation (10) gives:

$$\begin{bmatrix}\omega_3\\ \omega_4\end{bmatrix} = -(\widetilde{\mathbf{W}}_2^T\widetilde{\mathbf{W}}_2)^{-1}(\widetilde{\mathbf{W}}_2^T\widetilde{\mathbf{W}}_1)\begin{bmatrix}\omega_1\\ \omega_2\end{bmatrix}, \tag{11}$$

where the kinematic relationship matrix is $\mathbf{C}_{mode} = -(\widetilde{\mathbf{W}}_2^T\widetilde{\mathbf{W}}_2)^{-1}(\widetilde{\mathbf{W}}_2^T\widetilde{\mathbf{W}}_1)$.
In the case where $\boldsymbol{\omega}^{ext}$ contains speeds from ground nodes, the same idea holds after the following additional step: Since the speed of a ground node is always zero, columns of the matrix $\widetilde{\mathbf{W}}$ to be multiplied by the ground speed can be removed. Then, the definition of $\widetilde{\mathbf{W}}_1$ and $\widetilde{\mathbf{W}}_2$ must be modified as $[\widetilde{\mathbf{W}}_1, \widetilde{\mathbf{W}}_2, \widetilde{\mathbf{W}}_{gnd}] = \widetilde{\mathbf{W}}$ where $\widetilde{\mathbf{W}}_{gnd}$ are the columns to be removed. With that definition, Equation (11) holds for the cases that include ground nodes.

(ii) For pure electric configurations, if an engine exists in the configuration, the following definitions can be made $[\widetilde{\mathbf{W}}_{eng}, \widetilde{\mathbf{W}}_1, \widetilde{\mathbf{W}}_{gnd}] = \widetilde{\mathbf{W}}$, where $\widetilde{\mathbf{W}}_{eng}$ is the column multiplied by engine speed. Since the engine is always grounded in a pure electric configuration, i.e., it is always at zero speed, both $\widetilde{\mathbf{W}}_{eng}$ and $\widetilde{\mathbf{W}}_{gnd}$ can be removed. Then, linearly independent rows of $\widetilde{\mathbf{W}}_1$ are used to model the kinematic relationship of pure electric configurations. Note that while 1 to 3 dofs exist among the configurations generated by the process, we are only interested in kinematically 1-dof and 2-dof configurations. 3-dof configurations require a sophisticated control algorithm and they are not used in common practice. Therefore only $\widetilde{\mathbf{W}}_1$ matrices with ranks 1 and 2 are used for practicality. For a 1-dof configurations, the kinematic relationship matrix is defined as:

$$\begin{bmatrix}1\\ 0\end{bmatrix}\omega_2 = \mathbf{C}_{mode}\begin{bmatrix}\omega_3\\ \omega_4\end{bmatrix}. \tag{12}$$

Similarly, for a 2-dof configuration, the same kinematic matrix becomes:

$$\omega_2 = \mathbf{C}_{mode}\begin{bmatrix}\omega_3\\ \omega_4\end{bmatrix}. \tag{13}$$

4 Multi-mode Architectures

We create multi-mode architectures by combining two or more configurations under a single arrangement of its components. Recall that we call each particular configuration in a multi-mode architecture a *driving mode*. The main motivation to design multi-mode architectures is to benefit from switching among a variety of "specialized" modes, each of which operating efficiently under different driving conditions. For instance, a mode that is designed to operate in highway driving conditions is not necessarily efficient in city driving conditions. Incorporating the two in one powertrain can achieve better efficiency than a single mode designed for both driving conditions.

An example for an architecture with multiple modes is given in Figure 1. Switching among the modes is achieved by engaging or disengaging clutches. We represent every mode with a different modified bond graph. Since the number of clutches involved must be limited in practice, a systematic way to evaluate the required clutches for a multi-mode architecture is necessary during architecture design. In this section we will describe the process to calculate the clutching solutions for given three modes and then generalize to any number of modes.

4.1 Clutching Solutions

We introduced the connectivity table earlier in Section 2.2. A link must be formed between modified bond graph representation and connectivity table in order to automate the process of finding clutching solutions.

We explain the process of extracting this information from the modified bond graph using a color analogy. The weights around a 0-junction represents the kinematic relationships among sun, ring and carrier gears and every bond around 0-junction can be assigned to a different color representing each of these respective gears. In Figure 3, the edge

weights representing sun, ring and carrier gear are colored by red, green and blue, respectively. As seen in this figure, since the speeds around the 1-junction are the same, the same coloring is kept around a 1-junction. When this process is repeated for all bonds we can see the connection information of each external component by checking the color of the bond connecting an external component to its corresponding external junction. In case of a 2-PG mode, we need to start with 6 colors; for 3-PG modes we need 9 colors, and so on. When multiple 0-junctions impose different colors on a bond, i.e., when colors are mixed on a bond, it means this bond is connected to multiple PGs. Such color mixtures give information on the internal connections among PGs.

Once the connectivity table is extracted from the modified bond graph, one can calculate the number of clutches needed by comparing the connectivity tables of the driving modes to be combined. Basically adding or removing a connection requires one clutch and changing a connection of an external component from one gear to another requires two.

Figure 9 shows an example that compares connectivity tables of three 1-PG modes and identifies the clutches required. We perform a pairwise comparison of the modes in the architecture sequentially. Starting with modes A and B, in the figure, Mode B has an additional ground connected to the carrier that does not exist in Mode A. Adding this ground connection requires one clutch at the carrier gear. Also MG2 is connected to the ring gear in Mode A and connected to carrier gear in Mode B. Disconnecting MG2 from the ring requires a clutch at the ring and connecting it to the carrier requires another clutch at the carrier gear. Comparing modes B and C, we can see that engine and ground, which are connected in Mode B, are disconnected in Mode C. Disconnecting these components requires one clutch for each. We take the union of these clutches to calculate the final number. In this example we need four physical clutches to allow shifting among the three modes. These four clutches are located at the connections from (1) MG2 to R1, (2) MG2 to C1, (3) ground to C1, (4) engine to C1.

Note that this solution is independent from the order of the modes. If we follow the same steps switching from Mode A to Mode C and from Mode C to Mode B, we obtain the same set of clutches, for instance. These steps can be automated in an architecture design process.

5 Results

The formulation presented in this paper can be used to generate all possible configurations for systems with any number of PGs and any number of external components. In addition to the HEV modes, by removing the engine from the external components or connecting the engine and ground to the same gear, pure electric modes can also be generated.

The results we present in this section follow the causality assignment for external junctions discussed in Section 3.2. Recall that this assignment limits configurations to only power-split designs.

Also as discussed in Section 3.4, the rank of the matrix $\widetilde{\mathbf{W}}$ determines the kinematic degree of freedom of the configurations generated. In this section we present results for 2-dof hybrid configurations and both 1-dof and 2-dof pure electric configurations.

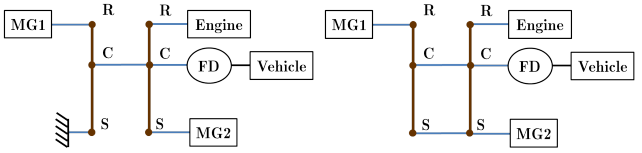

(a) First hybrid configuration (b) Second hybrid configuration

Fig. 10: All modes of the dual-mode architecture by Ai and Anderson [23]

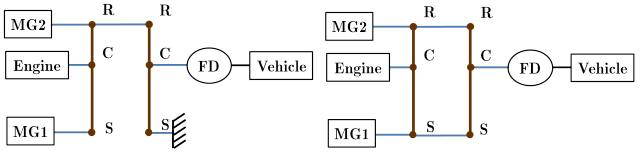

(a) First hybrid configuration (b) Second hybrid configuration

Fig. 11: All modes of the dual-mode architecture by Schmidt [40]

The process described above results in 52 unique configurations for one PG assuming one engine, two MGs, one ground and one vehicle output. Among these 52 configurations, 16 of them are hybrid and 36 are pure electric ones. The results include some available designs in the market such as hybrid and pure electric configurations of the Chevrolet Volt architecture shown in Figure 1.

The number of feasible configurations for 2-PG with the same powertrain components is 3420 where 2124 of them are hybrid and the rest 1296 are pure electric. Among these 2-PG configurations, there are some designs that look different but give the same quasi-static matrices $\mathbf{C}_{mode}$. Their graph representations are not isomorphic but are kinematically equivalent. When the gear ratio of the two PGs are both equal to 2, these 2124 hybrid configurations have 1178 unique kinematic matrices, for instance. These kinematically equivalent designs should not be eliminated in a design process since they might be useful for multi-mode architecture designs. For instance, two kinematically equivalent designs might result in different of number clutches needed in a multi-mode architecture. Also some of the configurations are only feasible when PG ratios are different. 36 of all 2-PG hybrid configurations give non-invertible $\mathbf{C}_{mode}$ matrices when two PG ratios are the same. The configuration in Figure 11b is an example to such configurations. When PG ratios are the same, the vehicle and engine speeds are imposed to be the same due to the kinematics of the both PG systems and thus dof of this hybrid configuration is reduced to 1. It appears as a non-invertible $\mathbf{C}_{mode}$ in this study.

The configuration generation process can create some available designs in the literature such as those by Ai and Anderson [23] given in Figure 10 and by Schmidt [40] given in Figure 11.

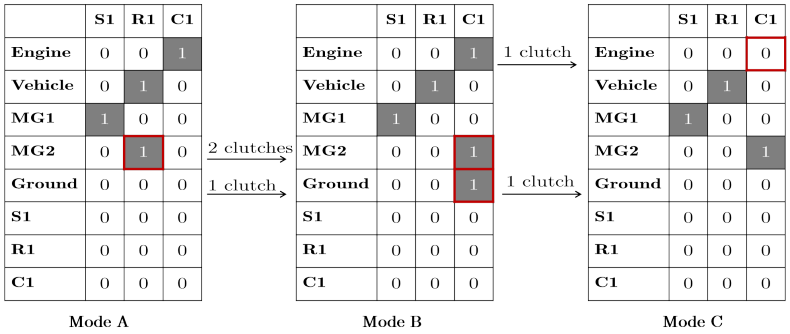

Fig. 9: Three sample connectivity tables and the corresponding clutching solution indicated by red boxes (best viewed in color)

6 Conclusions

In this paper we presented a formulation to generate all feasible hybrid and pure electric configurations relying on a modified bond graph representation. The formulation is general enough to be extended to any set of powertrain components and any number of PGs. We also presented the methodology to create multi-mode architectures using the modified bond graph representation of the generated designs. We identified sample designs among the generated configurations available in the literature.

The generation process can be integrated with a design evaluation and optimization framework to discover design architectures with improved fuel economy for a target vehicle application. Examples for such a design process can be found in [30, 31, 41]. These studies design the architecture and gear ratios in a hybrid powertrain by relying on a given set of feasible configurations such as the configurations generated in this study.

Acknowledgements

This research has been partially supported by General Motors Corp. and the Automotive Research Center, a US Army Center of Excellence in Modeling and Simulation of Ground Vehicle Systems headquartered at the University of Michigan. This support is gracefully acknowledged.

References

[1] Folkesson, A., Andersson, C., Alvfors, P., Alaküla, M., and Overgaard, L., 2003. "Real life testing of a hybrid pem fuel cell bus". *Journal of Power Sources,* **118**(1), pp. 349–357.

[2] Gao, D., Jin, Z., and Lu, Q., 2008. "Energy management strategy based on fuzzy logic for a fuel cell hybrid bus". *Journal of Power Sources,* **185**(1), pp. 311–317.

[3] Evans, D. G., Polom, M. E., Poulos, S. G., Van Maanen, K. D., and Zarger, T. H., 2003. Powertrain architecture and controls integration for gm's hybrid full-size pickup truck. Tech. rep., SAE Technical Paper.

[4] Lin, C.-C., Peng, H., Grizzle, J. W., and Kang, J.-M., 2003. "Power management strategy for a parallel hybrid electric truck". *Control Systems Technology, IEEE Transactions on,* **11**(6), pp. 839–849.

[5] Liu, J., 2007. "Modeling, configuration and control optimization of power-split hybrid vehicles". PhD dissertation, Dept. of Mechanical Engineering, The University of Michigan.

[6] Kicinger, R., Arciszewski, T., and Jong, K. D., 2005. "Evolutionary computation and structural design: A survey of the state-of-the-art". *Computers and Structures,* **83**(23), pp. 1943–1978.

[7] Bendsøe, M. P., and Kikuchi, N., 1988. "Generating optimal topologies in structural design using a homogenization method". *Computer methods in applied mechanics and engineering,* **71**(2), pp. 197–224.

[8] Roth, B., 1967. "Finite-position theory applied to mechanism synthesis". *Journal of Applied Mechanics,* **34**(3), pp. 599–605.

[9] Raghavan, M., 1989. "Analytical methods for designing linkages to match force specifications". PhD dissertation, Dept. of Mechanical Engineering, Stanford University.

[10] Koza, J. R., Bennett III, F. H., Andre, D., Keane, M. A., and Dunlap, F., 1997. "Automated synthesis of analog electrical circuits by means of genetic programming". *Evolutionary Computation, IEEE Transactions on,* **1**(2), pp. 109–128.

[11] Schneider, G., and Fechner, U., 2005. "Computer-based de novo design of drug-like molecules". *Nature Reviews Drug Discovery,* **4**(8), pp. 649–663.

[12] Wu, Z., Campbell, M. I., and Fernández, B. R., 2008. "Bond graph based automated modeling for computer-aided design of dynamic systems". *Journal of Mechanical Design,* **130**(4), p. 041102.

[13] Starling, A. C., and Shea, K., 2005. "A parallel grammar for simulation-driven mechanical design synthesis". In ASME 2005 International Design Engineering Technical Conferences and Computers and Information in Engineering Conference, ASME, Paper No: DETC2005-85414, pp. 427–436.

[14] Campbell, M. I., Cagan, J., and Kotovsky, K., 2000. "Agent-based synthesis of electromechanical design configurations". *Journal of Mechanical Design,* **122**(1), pp. 61–69.

[15] Hsieh, H.-I., and Tsai, L.-W., 1996. A methodology for enumeration of clutching sequences associated with epicyclic-type automatic transmission mechanisms. Tech. rep., SAE Technical Paper.

[16] Kahraman, A., Ligata, H., Kienzle, K., and Zini, D., 2004. "A kinematics and power flow analysis methodology for automatic transmission planetary gear trains". *Journal of Mechanical Design,* **126**(6), pp. 1071–1081.

[17] Conlon, B. M., Savagian, P. J., Holmes, A. G., Harpster, M. O., et al., 2011. Output split electrically-variable transmission with electric propulsion using one or two motors. US Patent 7,867,124.

[18] Sasaki, S., 1998. "Toyota's newly developed hybrid powertrain". In Proceedings of the 10th International Symposium on Power Semiconductor Devices and ICs, IEEE Press, pp. 17–22, doi:10.1109/ISPSD.1998.702540.

[19] Schmidt, M., 1996. Two-mode, split power, electromechanical transmission. US Patent 5,577,973.

[20] Schmidt, M., 1996. Two-mode, input-split, parallel, hybrid transmission. US Patent 5,558,588.

[21] Holmes, A., and Schmidt, M., 2002. Hybrid electric powertrain including a two-mode electrically variable transmission. US Patent 6,478,705.

[22] Holmes, A., Klemen, D., and Schmidt, M., 2003. Electrically variable transmission with selective input split, compound split, neutral and reverse modes. US Patent 6,527,658.

[23] Ai, X., and Anderson, S., 2005. "An electro-mechanical infinitely variable transmisson for hybrid electric vehicles". *SAE Technical Paper 2005-01-0281*.

[24] Schmidt, M., 1999. Two-mode, compound-split electro-mechanical vehicular transmission. US Patent 5,931,757.

[25] Raghavan, M., Bucknor, N. K., and Hendrickson, J. D., 2007. Electrically variable transmission having three interconnected planetary gear sets, two clutches and two brakes. US Patent 7,179,187.

[26] Zhang, X., Li, C.-T., Kum, D., and Peng, H., 2012. "Prius+ and volt- : Configuration analysis of power-split hybrid vehicles with a single planetary gear". *IEEE Transactions on Vehicular Technology,* **61**(8), pp. 3544–3552.

[27] Cheong, K. L., Li, P. Y., and Chase, T. R., 2011. "Optimal design of power-split transmissions for hydraulic hybrid passenger vehicles". In Proceedings of the 2011 American Control Conference, IEEE Press, pp. 3295–3300, doi:10.1109/ACC.2011.5991509.

[28] Zhang, X., Li, S. E., Peng, H., and Sun, J., 2015. "Efficient exhaustive search of power-split hybrid powertrains with multiple planetary gears and clutches". *Journal of Dynamic Systems, Measurement, and Control,* **137**(12), p. 121006.

[29] Bayrak, A. E., Ren, Y., and Papalambros, P. Y., 2013. "Design of hybrid-electric vehicle architecture using auto-generation of feasible driving modes". In Proceedings of the ASME 2013 International Design Engineering Technical Conferences, ASME, Paper No. DETC2013-13043.

[30] Bayrak, A. E., Kang, N., and Papalambros, P. Y., 2015. "Decomposition based design optimization of hybrid electric powertrain architectures: Simultaneous configuration and sizing design". *submitted to Journal of Mechanical Design*.

[31] Bayrak, A. E., Kang, N., and Papalambros, P. Y., 2015. "Decomposition-based design optimization of hybrid electric powertrain architectures: Simultaneous configuration and sizing design". In Proceedings of the ASME 2015 International Design Engineering Technical Conferences, ASME, Paper No. DETC2015-46861.

[32] Benford, H. L., and Leising, M. B., 1981. The lever analogy: A new tool in transmission analysis. Tech. rep., SAE Technical Paper.

[33] Chatterjee, G., and Tsai, L.-W., 1996. "Computer-aided sketching of epicyclic-type automatic transmission gear trains". *Journal of Mechanical Design,* **118**(3), pp. 405–411.

[34] Kim, N., Kim, J., and Kim, H., 2008. "Control strategy for a dual-mode electromechanical, infinitely variable transmission for hybrid electric vehicles". *Proceedings of the Institution of Mechanical Engineers, Part D: Journal of Automobile Engineering,* **222**(9), pp. 1587–1601.

[35] Karnopp, D. C., Margolis, D. L., and Rosenberg, R. C., 2012. *System Dynamics: Modeling, Simulation, and Control of Mechatronic Systems*, 5th ed. Wiley, Hoboken, NJ.

[36] Read, R. C., and Corneil, D. G., 1977. "The graph isomorphism disease". *Journal of Graph Theory,* **1**(4), pp. 339–363.

[37] Fortin, S., 1996. The graph isomorphism problem. Tech. rep., Technical Report 96-20, University of Alberta, Edomonton, Alberta, Canada.

[38] McKay, B. D., et al., 1981. *Practical graph isomorphism*. Department of Computer Science, Vanderbilt University.

[39] MATLAB, 2014. *graphisomorphism*. The MathWorks Inc., Natick, Massachusetts.

[40] Schmidt, M., 1999. Electro-mechanical powertrain. US Patent 5,935,035.

[41] Bayrak, A. E., 2015. "Topology considerations in hybrid electric vehicle powertrain architecture design". PhD dissertation, Dept. of Mechanical Engineering, The University of Michigan.